The Relationship Between Slag Structure, Sulphur Transport Through the Phase Boundary and Interfacial Tension Between Liquid Steel and Molten Slags

Prof. Dr.-Ing. Tarek El Gammal; Dr.rer.nat.
Erwin Wosch; Dipl.-Ing. Zhiyong Yang,
Institute for Ferrous Metallurgy, IEHK,
RWTH Aachen, Intzestraße 1, 52072
Aachen, Germany. Tel.: 0241/805790

ABSTRACT

This paper describes measured concentration profiles of sulphur in slags of the tree component system $CaO\text{-}Al_2O_3\text{-}CaF_2$ mathematically. The mass transfer of sulphur is calculated, which can be expressed in terms of the activation energy of sulphur diffusion. The activation energy has a direct relation to the slag structure. The results show that there is a direct connection between the slag structure, the transport mechanism and the interfacial tension of the two phases.

1. INTRODUCTION

The transfer of a dissolved element from a stagnant steel bath into a molten slag layer is at the beginning of the process controlled by the mechanism of the transport at and through the interface between the two phases. This is also valid for suspendet drops of one phase in the other, where mass exchange takes place.

To find the relationship between the slag structure, interfacial tension and the transport mechanism of sulphur from liquid steel into molten slags, two experimental series have been conducted. In the first run, the kinetics of sulphur transport from the liquid steel into the molten slag has been investigated. The sulphur concentration profiles were determined by microprobe and chemical analysis in the direction orthogonal to the phase boundary as a function of time. The detailed analysis of the profiles yields the information about the diffusion of sulphur in the slag. Interest has been focused on the slag layer adjacent to the interface. In the second one the interfacial tension between the two phases has been determined using the drop detachment method.

2. EXPERIMENTAL PROCEDURE

2.1 Determination of sulphur concentration profiles in the slag

To investigate the mass transfer of desulphurization, concentration profiles of sulphur in non-stirred steel-slag systems were determined experimentally. Buoyancy-driven convection was suppressed by locating the samples in the temperature constant zone of a Tammann furnace, and by choosing an appropriate crucible geometry. The aspect ratio of the crucible was 0.008m / 0.1m=0.08.

The steel samples (Ck45), with initial sulphur contents of 0.11% and 0.13%, and the prefused slags of the tree component system $CaO\text{-}Al_2O_3\text{-}CaF_2$ were introduced in the gas-tight Tammann furnace, previously flooded with argon. The chemical compositions of the slags are given in table I. The viscosities of the slags were taken from literature[1,2].

Figure 1 shows the special constructional features of the crucibles. A perforated graphite disc was served as retainer ring for eight sintered Al_2O_3 crucibles. The slag and steel samples were separated by a graphide stamp, to prevent their contact during melting on.

After melting of the samples, the slag is added by lifting the stamps at prescribed intervals. This gave reaction times of 3, 8, 13 and 18 minutes. The samples were then rapidly cooled under argon flow, and the sulphur profiles in the slag phase determined by microprobe and chemical analysis. Several experimantal series in the temperature range beween 1520°C and 1600°C have been carried out (see table II).

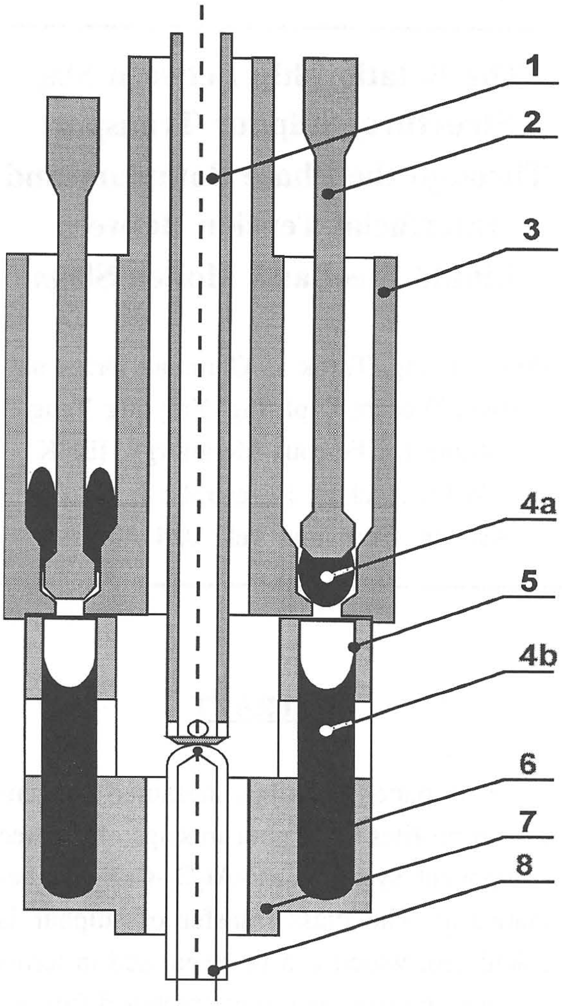

Fig. 1 Crucible for measurement of sulphur concentration profiles; 1: quenching-gas lance, 2: graphide stamp, 3: graphide crucible, 4a,b: slag sample, 5: sintered Al_2O_3 crucible, 6: steel sample, 7: graphide retainer ring, 8: thermocouple.

Table I Chemical compositions and viscosities of the slags used

No.	CaO wt %	Al_2O_3 wt %	CaF_2 wt %	η 1520°C kg/(m•s)	η 1560°C kg/(m•s)	η 1600°C kg/(m•s)
1	50	50	0	0.419	0.358	0.3
2	50	40	10	0.213	0.181	0.15
3	50	35	15	0.154	0.122	0.092
4	50	30	20	0.111	0.093	0.076
5	50	25	25	0.093	0.078	0.064

1.2 Determination of Interfacial tension

The slags were prepared from a synthetic mixture and prefused also in a vacuum-tight Tammann furnace under argon atmosphere, using graphite crucibles. The boiling effect at reduced pressure promoted homogeneous mixing of the slag components. The interfacial tension was determined according to the drop detachment method. Figure 2 shows the experimental set up. This method requires only a simple testing apparatus and yields good reproducible results. Its successful application has often been demonstrated[3..11)].

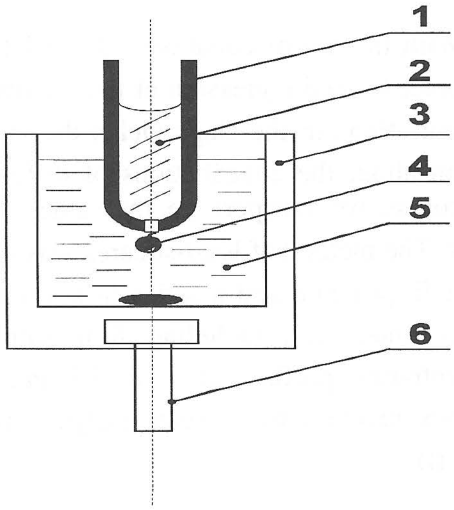

Figure 2 Experimental set up for interfacial tension measurement; 1: capillary, 2: steel sample, 3: graphite crucible, 4: detaching drop, 5: liquid slag, 6: balance.

Before applying the drop detachment method to determine interfacial tension, it must be established that no chemical reaction or mass transfer takes place between steel and slag, since this would falsify the results. Analysis of steel and slag before and after the experiments did not show any changes in their chemical compositions.

3. DETERMINATION OF INTERDIFFUSIVITY

At the metal/slag interface, the measured sulphur concentrations increase exponentially with time. If in the slag a system of cartesian coordinates is so defined that **x≥0** is the distance from the phase boundary, the sulphur concentration at the interface **(S)*** can be written as:

$$\begin{aligned}(S)_{for\ x=0} &= (S)^* \\ &= a \cdot (1-e^{-bt}) + (S)_0 \\ with:\ a &= (S)_E - (S)_0 \qquad \{1\}\end{aligned}$$

Where **t** denotes the time, **a** the difference between the equilibrium and the initial sulphur concentration in the slag and **b** the sulphur absorption rate. Figure 3 shows some examples of measured sulphur concentrations in the slag at the metal/slag interface as a function of time.

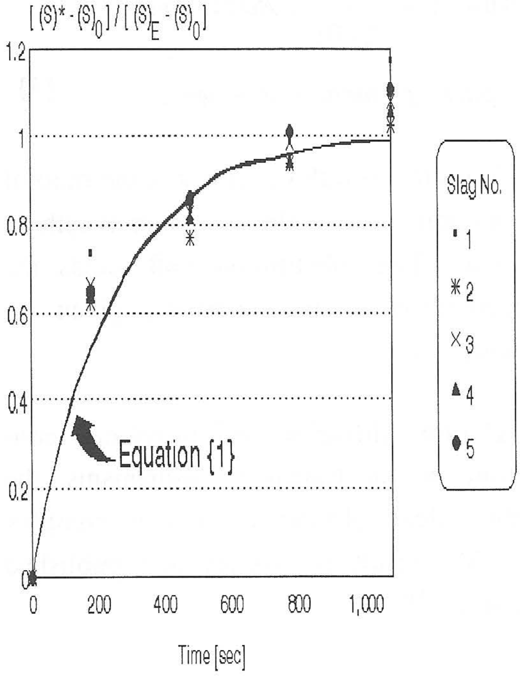

Fig. 3 Measured sulphur concentrations at the interphase as a function of time (normalized).

The sulphur transport in the slag near the metal/slag interface may occur by diffusion and interfacial convection. In the case that only diffusion acts as transport mechanism, the sulphur concentration as a function of time and place can be expressed by Fick's second law:

$$\frac{\partial (S)}{\partial t} = D \cdot \frac{\partial^2 (S)}{\partial x^2} \qquad \{2\}$$

The diffusion coefficient **D** is assumed to be constant. To determine the sulphur concentration in the slag, this partial differential equation has to be solved on the condition given by equation {1}. This may be done at different ways, e.g. by the method of Laplace-transformation[12)] (for more details see appendix). The solution is:

$$(S) = (S)_0 + a \cdot \left[erfc(z) - e^{-bt} \cdot \cdot Re\left(e^{ix\sqrt{\frac{b}{D}}} \cdot erfc(z + i\sqrt{bt}) \right) \right]$$

$$with{:}\ z = \frac{x}{2\sqrt{Dt}}\ ,\ Re(z) = real\ part\ of\ complex\ number\ z \qquad \{3\}$$

The dimensionless value **z** is the ratio of the **x**-coordinate to the diffusion length in the slag. The substitution **x=0** yields the concentration at the interface, given by equation {1}.

If both, diffusion and interfacial convection, act as transport mechanisms, the mathematical solution has a more complex form. The result has already been published elsewere[13,14)]:

$$(S) = (S)_0 - a \cdot \{ erfc(z) \cdot \exp(2zw - w^2) - \frac{1}{2}[erfc(z+w) \cdot \exp(4zw) + erfc(z-w)] \}$$

$$with{:}\ z = \frac{x}{2\sqrt{Dt}}\ ,\ w = \frac{vt}{2\sqrt{Dt}} \qquad \{4\}$$

Where **w** denotes the ratio of convection length to diffusion length and **v** is the time- and space-averaged value of the convection velocity orthogonal to the interface. The sulphur concentration at the interface (**x=0**) also takes on the exponential profile given by equation {1}.

With the aid of equations {3} and {4}, computer backed regression of the measured concentrations in the slags yields the information about the contributions of diffusive and convective transport, i.e. the values of **D** and **v**. The method of least-squares was used in the fit program and a series of seventeen experiments, each including four sulphur concentration profiles of 3, 8, 13 and 18 minutes reaction time were analysed (see table II).

The analyses of all profiles show that the mass transfer in the steel/slag systems investigated is predominantly governed by diffusion. Within the limits of experimental accuracy, the concentration profiles follow the solution of Fick's second law given by equation {3}. Figure 4 shows a selection of measured and calculated plots for the slag no. 3 after 8 minutes at three different temperatures.

Table II The interdiffusivity in the slag, as determined under various experimental conditions, all data are given in SI units, i.e. **D** is given in m²/s, to convert **D** from metric to English units multiply the values in the table with the factor $1.549996 \cdot 10^3$ in²/s, the first column refers to the CaF_2 content of the slags (table I), at the temperatures T_1, T_3 and T_4 the initial sulphur content of the steel is: $[S]_0=0.11\%$ and at the temperature T_2: $[S]_0=0.13\%$.

CaF_2 in wt %	T_1 1520°C	T_2 1550°C	T_3 1560°C	T_4 1600°C
0	$1.8 \cdot 10^{-9}$	$2.4 \cdot 10^{-9}$	$3.6 \cdot 10^{-9}$	$21 \cdot 10^{-9}$
10	$3.0 \cdot 10^{-9}$	$11 \cdot 10^{-9}$	$18 \cdot 10^{-9}$	$38 \cdot 10^{-9}$
15	$29 \cdot 10^{-9}$	$37 \cdot 10^{-9}$	$47 \cdot 10^{-9}$	$83 \cdot 10^{-9}$
20	-	$51 \cdot 10^{-9}$	-	-
25	$50 \cdot 10^{-9}$	$57 \cdot 10^{-9}$	$75 \cdot 10^{-9}$	$80 \cdot 10^{-9}$

Table III Measured equilibrium sulphur concentrations S_E given in weight-% and the sulphur absorption rate **b** given in 1/s, as determined under various experimental conditions, the first column refers to the CaF_2 content of the slags (table I), at the temperatures T_1, T_3 and T_4 the initial sulphur content of the steel is: $[S]_0=0.11\%$ and at the temperature T_2: $[S]_0=0.13\%$.

CaF_2 in wt %	T_1 1520°C	T_2 1550°C	T_3 1560°C	T_4 1600°C
		b in 1/s		
0	$1.70 \cdot 10^{-3}$	$4.00 \cdot 10^{-3}$	$2.40 \cdot 10^{-3}$	$3.50 \cdot 10^{-3}$
10	$1.75 \cdot 10^{-3}$	$4.04 \cdot 10^{-3}$	$2.60 \cdot 10^{-3}$	$3.50 \cdot 10^{-3}$
15	$1.80 \cdot 10^{-3}$	$4.05 \cdot 10^{-3}$	$2.70 \cdot 10^{-3}$	$3.85 \cdot 10^{-3}$
20	-	$4.07 \cdot 10^{-3}$	-	-
25	$1.90 \cdot 10^{-3}$	$4.10 \cdot 10^{-3}$	$3.00 \cdot 10^{-3}$	$3.90 \cdot 10^{-3}$
		S_E in wt %		
0	0.285	0.300	0.290	0.295
10	0.320	0.340	0.325	0.330
15	0.350	0.376	0.360	0.370
20	-	0.404	-	-
25	0.390	0.420	0.400	0.410

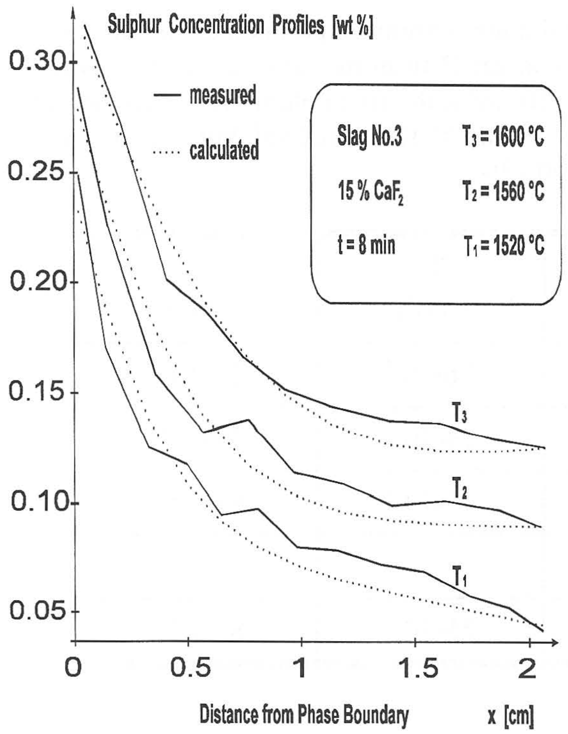

Fig. 4 Examples of measured and calculated sulphur concentration profiles.

The diffusion coefficients of sulphur, or more precise the interdiffusivities of sulphur in the slags[15], are listed in table II. The initial sulphur content of the steel at $\mathbf{T_1}$, $\mathbf{T_3}$, $\mathbf{T_4}$ is: $[S]_0=0.11\%$ and at $\mathbf{T_2}$: $[S]_0=0.13\%$. Slag no. 4 (20% CaF_2) was only examined at 1550°C and an initial sulphur content of the steel of 0.13%. An influence of $[S]_0$ on the interdiffusivity cannot be observed (see also fig. 5). As expected, greater interdiffusivities are reached with higher CaF_2 concentrations in the slag and at higher temperatures.

The values obtained for the equilibrium sulphur concentration $\mathbf{S_E}$ and the sulphur absorption rate **b** are shown in table III. Note that the equilibrium sulphur concentrations and the sulphur absorption rates of the experiments with $[S]_0=0.13\%$ are higher than the data given for $[S]_0=0.11\%$.

4. DETERMINATION OF ACTIVATION ENERGY OF DIFFUSION

The temperature dependence of the diffusion coefficient can be described by[15,16]:

$$D = D_0 \cdot e^{-\frac{\Delta E}{R \cdot T}} \qquad \{5\}$$

Where ΔE denotes the activation energy of diffusion and **T** the temperature. $\mathbf{D_0}$ and **R** (8.314 J/ (K•mol)) are constants. The activation energy of diffusion depends on the slag structure. In Figure 5 the logarithm of the interdiffusivity is ploted as a function of the CaF_2 contents and the inverse of temperature. From the slope of the linear regression, the activation energy of diffusion is calculated. The results are given in figure 6. Between 10% and 15% CaF_2, the activation energy of diffusion shows a marked drop, which indicates a change in the slag structure. In the same concentration intervall a drop of melting temperature and viscosity is observed.

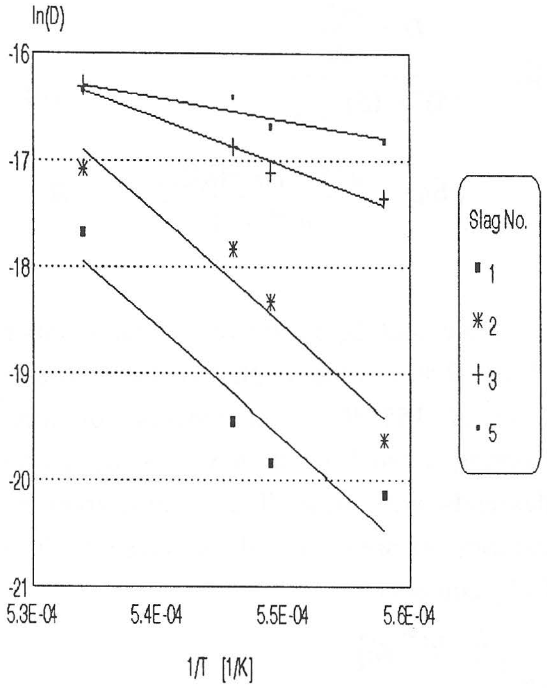

Fig. 5 Measured interdiffusivities as a function of 1/T.

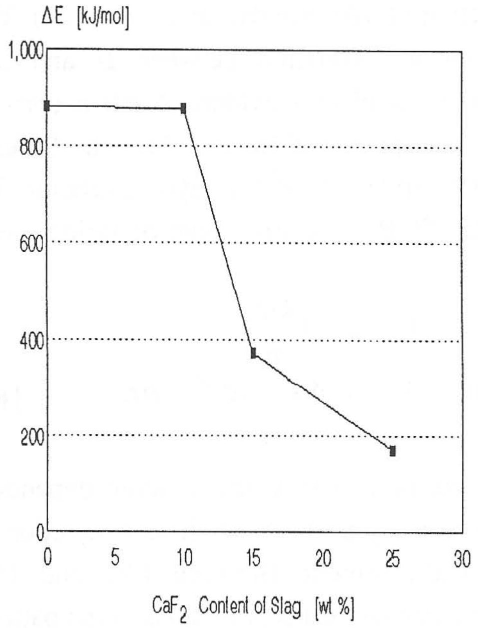

Fig. 6 Activation energy of diffusion of the slags used.

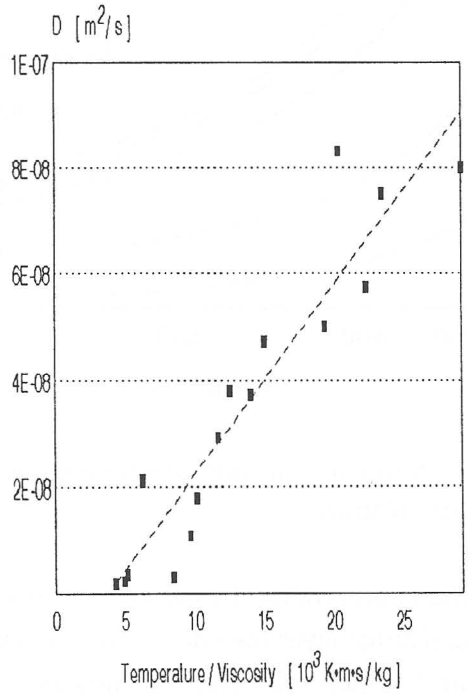

Fig. 7 Statistical correlation between the interdiffusivity and the quotient of T/η.

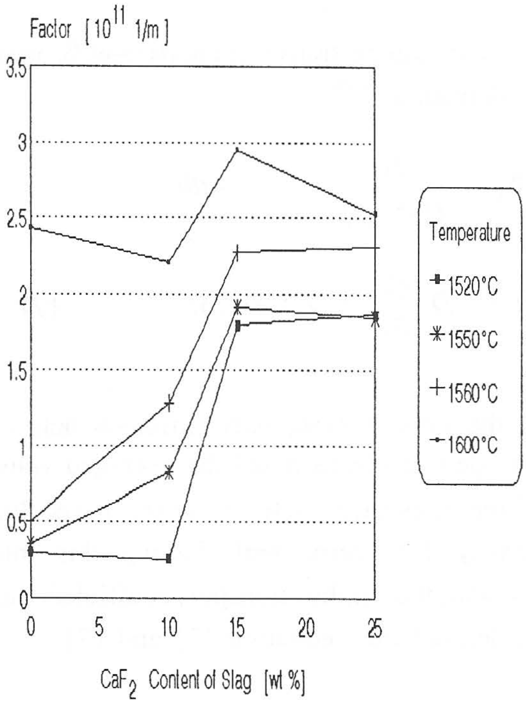

Fig. 8 Factor α in the Stokes-Einstein-/Eyring-relation as a function of CaF_2 contents of the slags.

Figure 7 gives the interdiffusivity as a function of T/η (η= dynamic viscosity). The statistical correlation between **D** and this quotient is clearly evident. Such a correlation is expected if for the slags the Stokes-Einstein-relation or the Eyring-relation are valid[17,18]. Both relations can be written as:

$$D = \alpha \cdot \left(\frac{k \cdot T}{\eta}\right) \quad , \qquad with: \; k = 1.381 \cdot 10^{-23} \; J/K \qquad \{6\}$$

The constant α is a slag strucure dependent quantity. Figure 8 shows it as a function of the CaF_2 content. Between 10% and 15% CaF_2, this factor takes on a stepwise pattern, which indicates a change in the slag structure, too.

5. DETERMINATION OF SULPHUR TRANSPORT COEFFICIENT

The sulphur transport coefficient β_S may be defined as[14,19]:

$$\beta_S = \frac{j_{|x=0}}{(S)^* - (S)_{|x\to\infty}} \quad , \; with:$$

$$j = -D \frac{\partial(S)}{\partial x} + v \cdot \{(S) - (S)_0\} \qquad \{7\}$$

In the present case, only diffusion acts as transport mechanism and the averaged value of the convection velocity in the mass flux density **j** is zero: **v=0**. Taking this into account, the sulphur transport coefficient can be derived from equation {3} and {7}:

$$\beta_S = \frac{-D \cdot \frac{\partial(S)}{\partial x}}{(S)^* - (S)_{|\,x\to\infty}} \qquad \{8\}$$

$$= \sqrt{b \cdot D} \cdot \frac{e^{-bt} \cdot i \cdot erf(i\sqrt{bt})}{e^{-bt} - 1} \quad , \in \Re$$

Note that β_S is always a real number. Figure 9 shows the sulphur transport coefficient at 1550°C as a function of time. Coming down from high values, β_S rapidly descends with time. The highest transport coefficients are observed for slags with high CaF_2 contents.

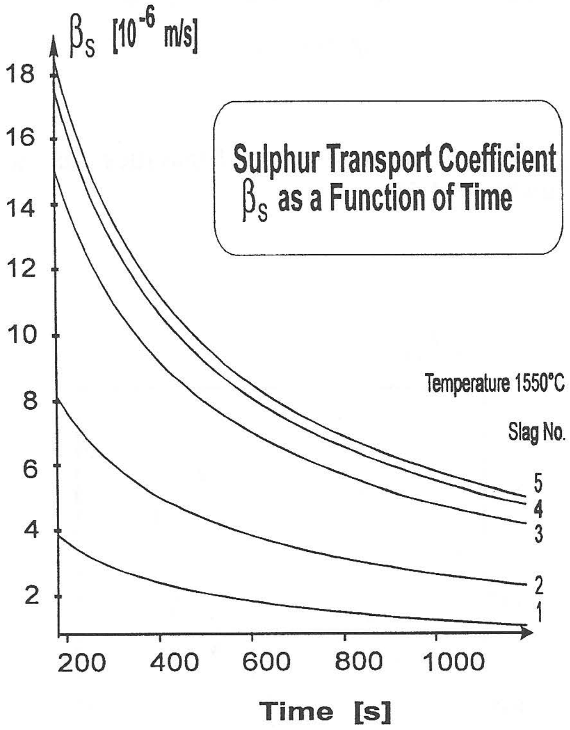

Fig. 9 Sulphur transport coefficient as a function of time.

The concentration boundary layer thicknes δ_N (Nernst layer thicknes, diffusion layer thicknes) is defined either by equation {9} or by equation {10}, depending on the model considered[19,20]:

$$\delta_N = \frac{D}{\beta_S} \qquad \{9\}$$

$$\delta_N = \sqrt{\pi \cdot Dt} \qquad \{10\}$$

Equation {10} is usually used as an approximation. Figure 10 gives δ_N calculated by both equations as a function of time at 1550°C. The Nernst layer thicknes calculated by the approximation exceeds the values form equation {9} by a factor of 1.5.

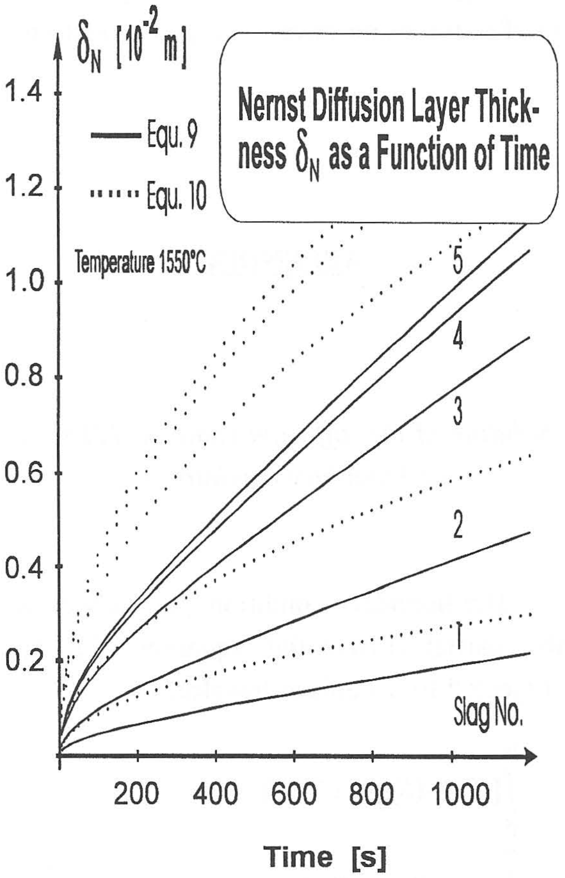

Fig. 10 Nernst layer thicknes δ_N as a function of time.

6. RELATIONSHIP BETWEEN INTERFACIAL TENSION AND ACTIVATION ENERGY

The results of the interfacial tension measurement between steel (Ck45) and slag also exhibit a characteristic drop above a definite CaF_2 content of the slag. Figure 11 shows the interfacial tension as a function of temperature and the quotient of CaF_2/Al_2O_3. The measured values decrease rapidly at CaF_2 / Al_2O_3=0.4. Between 1500°C and 1600°C the temperature dependence of the interfacial tension follows a simple linear law.

The relationship between the interfacial tension and the activation energy of diffusion is given in figure 12. Both, the interfacial tension and the activation energy of diffusion approximately follow a parallel course. This shows that slag structure, sulphur transport and interfacial tension are strongly associated.

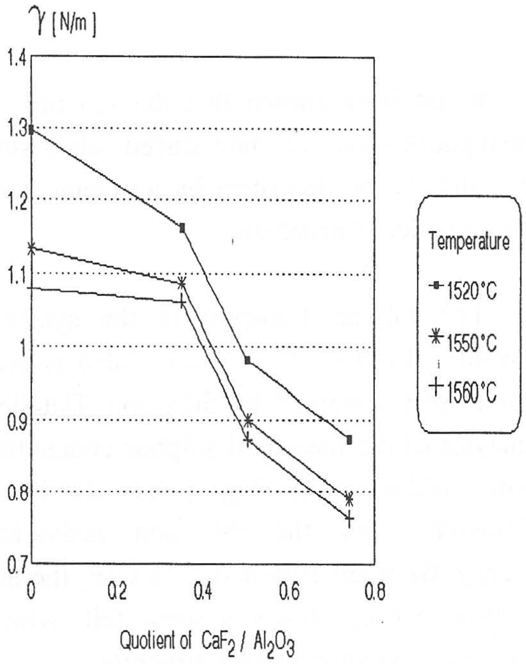

Fig. 11 Measured interfacial tension between steel (Ck45) and slag as a function of temperature and the quotient CaF_2/Al_2O_3.

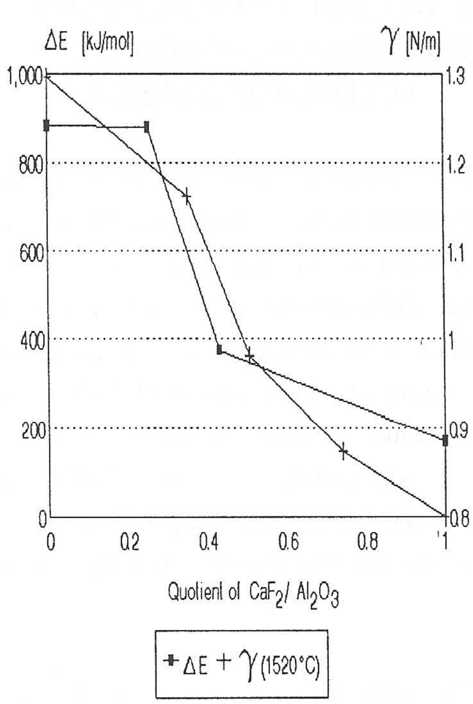

Fig. 12 Relationship between interfacial tension an diffusion activation energy as a function of CaF_2/Al_2O_3.

7. CONCLUSION

It has been shown that the kinetics of desulphurization of non-stirred steel-slag systems can be described by an elementary mathematical formalism.

The sulphur transport in the systems considered (Ck45, CaO-Al_2O_3-CaF_2) is predominantly governed by diffusion. Detailed analysis of the measured sulphur concentration profiles in the slags yields the interdiffusivity and the diffusion activation energy. Between 10% and 15% CaF_2 the activation energy shows a steep fall, which indicates a change in slag structure.

The slags used, statistically satisfy the Stokes-Einstein-/Eyring-relation. The sulphur transport coefficient rapidly descends with time and the highest values are observed for slags with high CaF_2 contents. These slags also reach the highest values of the Nernst diffusion layer thickness.

The measured interfacial tensions show a characteristic drop above a definite CaF_2 content. Interfacial tension and activation energy of diffusion follow a parallel course and slag structure, sulphur transport and interfacial tension have a strong correlation.

APPENDIX

Solution of the diffusion equation {2} with the boundary condition {1}

The boundary condition {1}, as well as the partial differential equation {2}, are subjected to a Laplace-transform:

$$\int_0^\infty [(S)^* - (S)_0] \cdot e^{-pt}\, dt =$$

$$a \cdot \int_0^\infty (1 - e^{-bt}) \cdot e^{-pt}\, dt \qquad \Rightarrow$$

$$\overline{(S)^*} - \frac{(S)_0}{p} = a \cdot \left(\frac{1}{p} - \frac{1}{p+b}\right) , \quad \{A1\}$$

$$\int_0^\infty e^{-pt} \cdot \frac{\partial (S)}{\partial t}\, dt = D \cdot \frac{\partial^2}{\partial x^2} \int_0^\infty e^{-pt} \cdot (S)\, dt$$

$$e^{-pt}\,(S)\Big|_0^\infty + p \int_0^\infty e^{-pt}\,(S)\, dt = D\,\frac{\partial^2}{\partial x^2} \int_0^\infty e^{-pt}\,(S)\, dt \quad \Rightarrow$$

$$-(S)_0 + p\,\overline{(S)} = D\,\frac{\partial^2}{\partial x^2}\overline{(S)}\,, \qquad \{A2\}$$

Where p is the Laplace-transformation parameter. The differential equation {A2} can be solved easily, giving:

$$\overline{(S)} = A(p) \cdot e^{-\sqrt{\frac{p}{D}} \cdot x} + \frac{(S)_0}{p} \qquad \{A3\}$$

A(p) follows from equation {A1} and {A3} by:

$$\overline{(S)}\Big|_{x=0} = \overline{(S)^*} = A(p) + \frac{(S)_0}{p}$$

$$\overline{(S)^*} = a \cdot \left(\frac{1}{p} - \frac{1}{p+b}\right) + \frac{(S)_0}{p}$$

$$A(p) = a \cdot \left(\frac{1}{p} - \frac{1}{p+b}\right) \qquad \{A4\}$$

Substitution of A(p) in equation {A3} yields the Laplace-transformed sulphur concentration in the slag:

$$\overline{(S)} = a \cdot \left(\frac{1}{p} - \frac{1}{p+b}\right) \cdot e^{-\sqrt{\frac{p}{D}} \cdot x} + \frac{(S)_0}{p}\,, \qquad \{A5\}$$

The inverse transformation yields for the slag:

$$(S) = (S)_0 + a \cdot \Big[\, erfc(z) - e^{-bt} \cdot Re\big(e^{ix\sqrt{\frac{b}{D}}} \cdot erfc(z + i\sqrt{bt})\, \big) \Big]$$

$$with:\; z = \frac{x}{2\sqrt{Dt}}\,, \qquad \{\,A6\,\}$$

Re(z)=real part of complex number z

REFERENCES

1) Mills, K. C.; Keene, B. J.: Physicochemical properties of molten CaF_2-based slags, International Metals Reviews, 1981, No. 1, p. 21/69.

2) Chen, J. X.: Handbook of tables and data for steelmaking, Metallurgical Publishing, Beijing, PR China (1984).

3) El Gammal, T.; Müllenberg, R. D.: Arch. Eisenhüttenwesen 51, 1980, Nr.6, p.221/26.

4) El Gammal, T.; Mayer, O. R.: Molten Salt Chem. and Techn., Kyoto, 1983, p.239/42.

5) Keskinen, K.; Taskinen, A.; Lilius, K.: Scand. J. Metall. 13, 1984, Nr.1, p.11/14.

6) Keskinen, K.; El Gammal, T.: Erzmetall 40, 1987, Nr.6, p. 312/16.

7) El Gammal, T.; Stracke, P.: Int. Symp. Near Net Shape Products, 13th-17th Nov., 1988, Honolulu, p. 693/704.

8) El Gammal, T.; Stracke, P.: 3rd Int. Conf. Molten Slags & Fluxes, 27th-29th June, 1989, Strathclyde, p.207/14.

9) El Gammal, T.; Hinds, G.; Schoneberg, U.: steel research 62, no. 4, (1991), p. 152/156.

10) El Gammal, T.; Schoneberg, U.: Stahl und Eisen 112, 1992, Nr.1, p. 45/9.

11) El Gammal, T.; Schrinner, H.-J.; Wosch, E.: Influence of Carbon, Silicon, and Molybdenum on the Separating and Emulsifying Behaviour of Steel and Slag; steel research 67, no. 4, (1996), p. 138/143.

12) Crank, J.: The Mathematics of Diffusion, 2nd ed., Clarendon Press, Oxford (1975).

13) El Gammal, T.; Lim, B.-M.; Wosch, E.: The Mechanism of Sulphur Movement into the Molten Slag Phase from Liquid Steel; Proc. 4th International Conference on Molten Slags and Fluxes, ISIJ, Sendai, Japan, (1992), p. 292/97.

14) El Gammal, T.; Wosch, E.; Lim, B.-M.: Concentration Profiles of Iron and Sulphur in Non-Stirred Steel-Slag Systems; steel research 66, no. 8, (1995), p. 331/7.

15) Turkdogan, E.T.: Physicochemical Properties of Molten Slags and Glasses, The Metals Society, London, 1983.

16) Bodsworth, C.: Physical Chemistry of Iron and Steel Manufacture, London & Colchester, (1963).

17) Atkins, P. W.: Physical Chemistry, 5th ed., Oxford University Press, Oxford (1994), p. 795.

18) Eyring, H.: Journal of Chemical Physics, 4 (1936), p.283.

19) Oeters, F.: Metallurgie der Stahlherstellung, Springer Verlag, Düsseldorf (1989).

20) Nernst, W.: Theorie der Reaktionsgeschwindigkeit in heterogenen Systemen, Z. Phys. Chem. 47 (1904), p. 52/55.